Multi-Agent Systems in Smart Environments

from sensor networks to aerial platform formations

Giulia Michieletto

Ph.D. advisor: Angelo Cenedese

Dept. of Information Engineering
University of Padova

February 22, 2018

Multi-Agent Systems in **Smart Environments**

[www.yourstory.com]

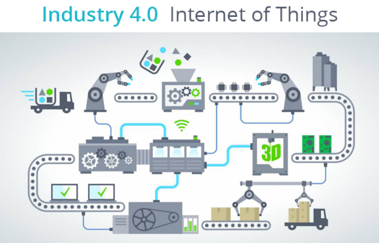

[www.mobinius.com]

[www.domotics.sg]

[zolertia.io]

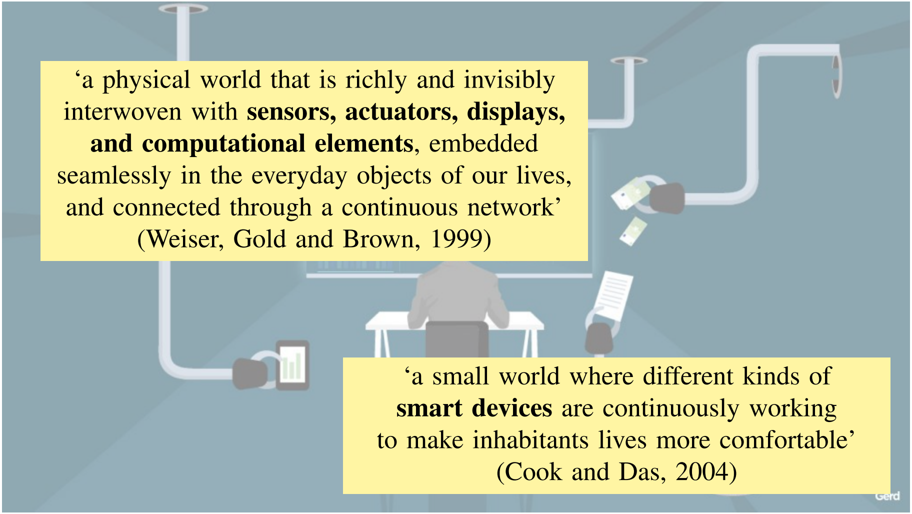

‘a physical world that is richly and invisibly interwoven with **sensors, actuators, displays, and computational elements**, embedded seamlessly in the everyday objects of our lives, and connected through a continuous network’ (Weiser, Gold and Brown, 1999)

‘a small world where different kinds of **smart devices** are continuously working to make inhabitants lives more comfortable’ (Cook and Das, 2004)

[www.tapscape.com]

Multi-Agent Systems in Smart Environments

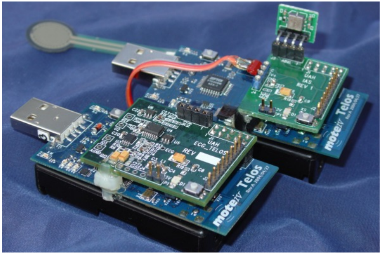

[www.ece.uah.edu]

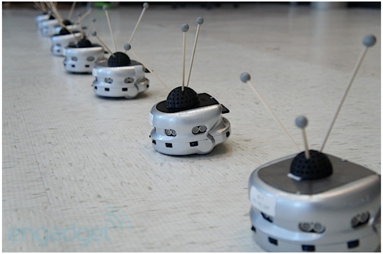

[www.engadget.com]

[newyork.cbslocal.com]

[optitrack.com]

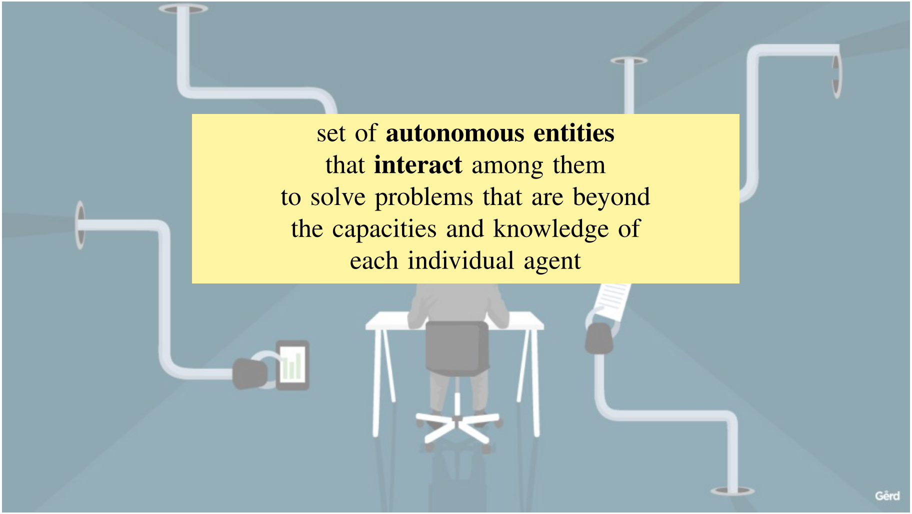

set of **autonomous entities**
that **interact** among them
to solve problems that are beyond
the capacities and knowledge of
each individual agent

[www.tapscape.com]

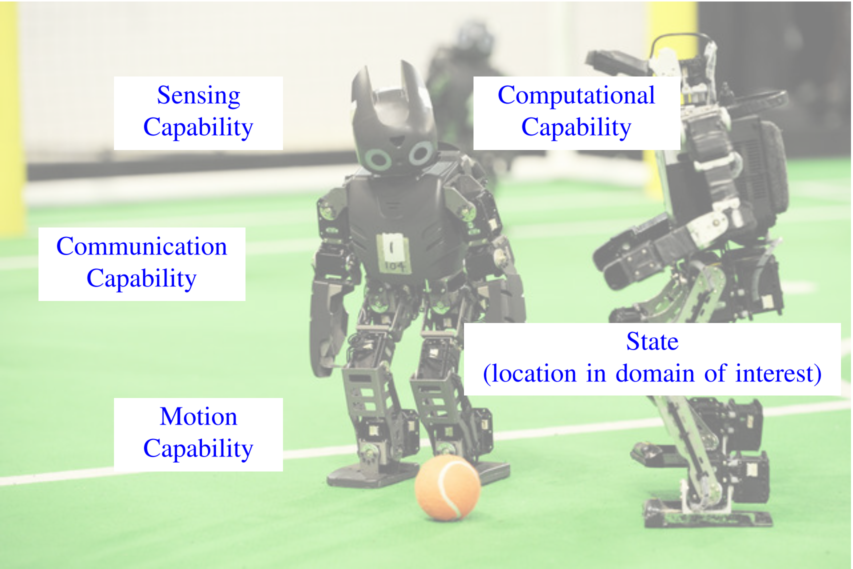
Sensing
Capability
Computational
Capability
Communication
Capability
State
(location in domain of interest)
Motion
Capability

[avax.news]

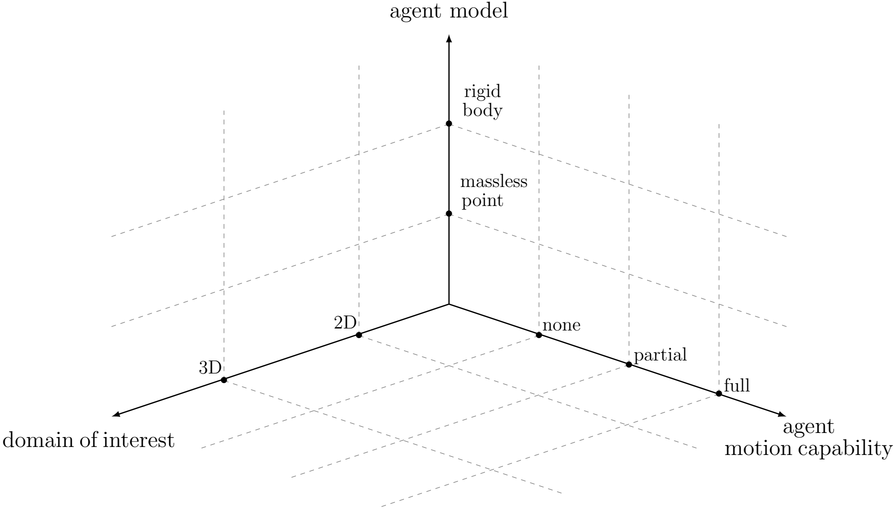
agent model
rigid
body
massless
point
2D
3D
none
partial
full
domain of interest
agent
motion capability

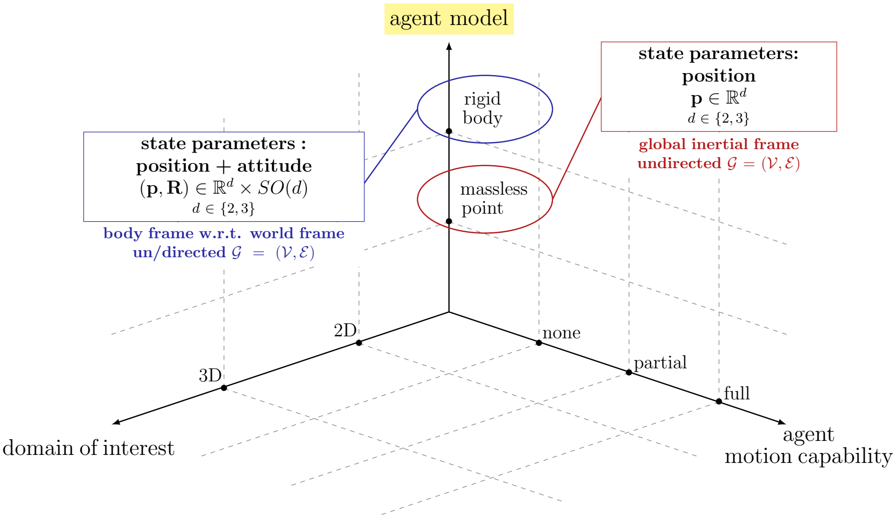
agent model
state parameters:
position
$\mathbf{p} \in \mathbb{R}^d$
$d \in \{2,3\}$
global inertial frame
undirected $\mathcal{G} = (\mathcal{V}, \mathcal{E})$
rigid body
massless point
state parameters :
position + attitude
$(\mathbf{p}, \mathbf{R}) \in \mathbb{R}^d \times SO(d)$
$d \in \{2,3\}$
body frame w.r.t. world frame
un/directed $\mathcal{G} = (\mathcal{V}, \mathcal{E})$
2D
3D
none
partial
full
domain of interest
agent
motion capability

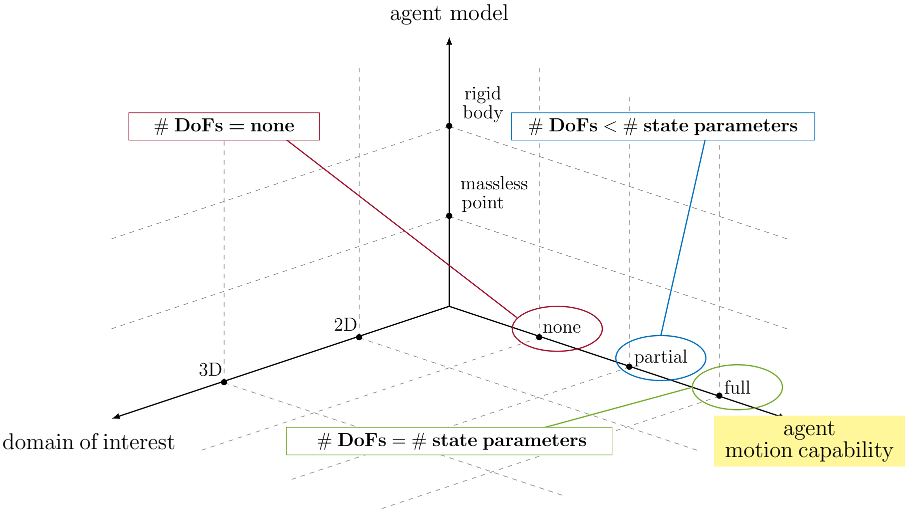

agent model
rigid body
massless point
DoFs = none
DoFs < # state parameters
2D
3D
none
partial
full
domain of interest
DoFs = # state parameters
agent motion capability

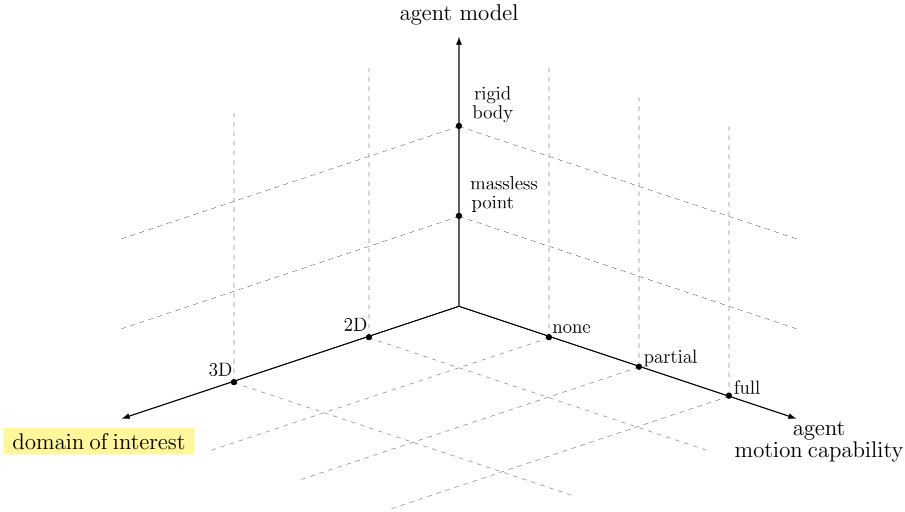
agent model
rigid
body
massless
point
2D
3D
none
partial
full
domain of interest
agent
motion capability

Research direction

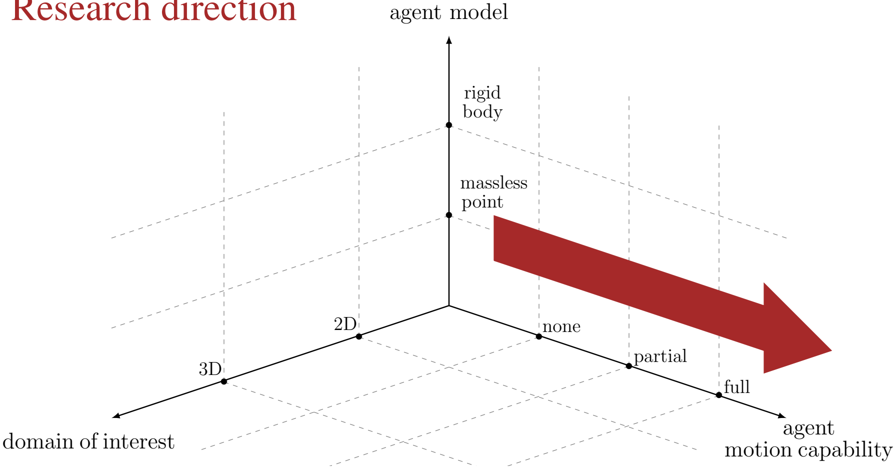

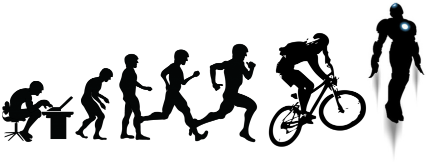

WSNs - Wireless Sensor Networks

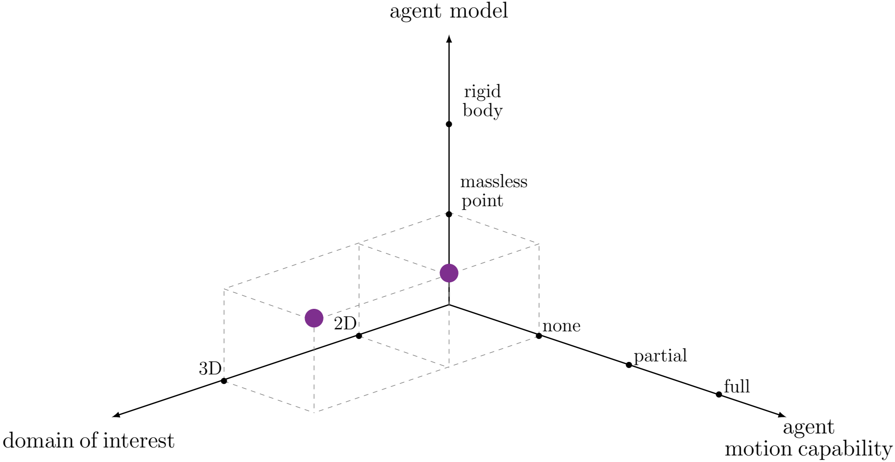

WSNs - Wireless Sensor Networks

large number of
compact and cheap devices
deployed in an area of interest

system state: $\{\mathbf{p}_i \in \mathbb{R}^d\}_{i=1}^n$

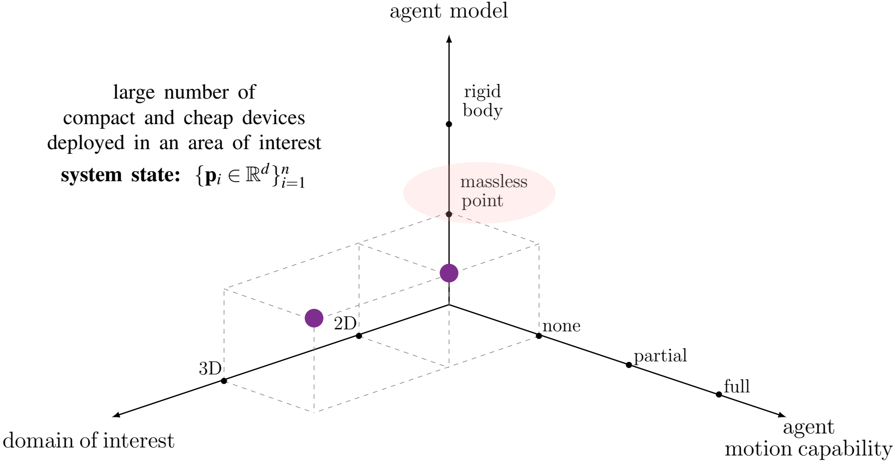

WSNs - Wireless Sensor Networks

large number of
compact and cheap devices
deployed in an area of interest

system state: $\{\mathbf{p}_i \in \mathbb{R}^d\}_{i=1}^n$

local sensing data
from environment

measurements: $\{m_i \in \mathbb{R}\}_{i=1}^n$

measurements exchange
according to
communication capabilities

$\mathcal{G} = (\mathcal{V}, \mathcal{E})$

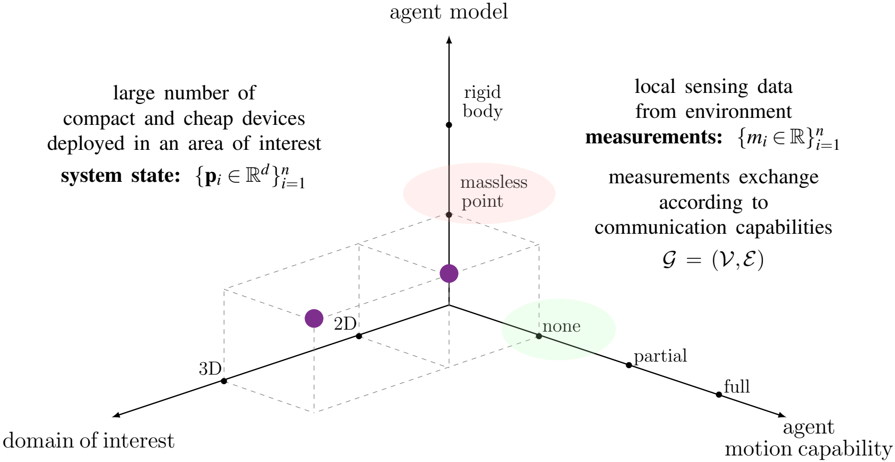

WSNs - Wireless Sensor Networks

large number of
compact and cheap devices
deployed in an area of interest
system state: $\{\mathbf{p}_i \in \mathbb{R}^d\}_{i=1}^n$

local sensing data
from environment
measurements: $\{m_i \in \mathbb{R}\}_{i=1}^n$

measurements exchange
according to
communication capabilities
$\mathcal{G} = (\mathcal{V}, \mathcal{E})$

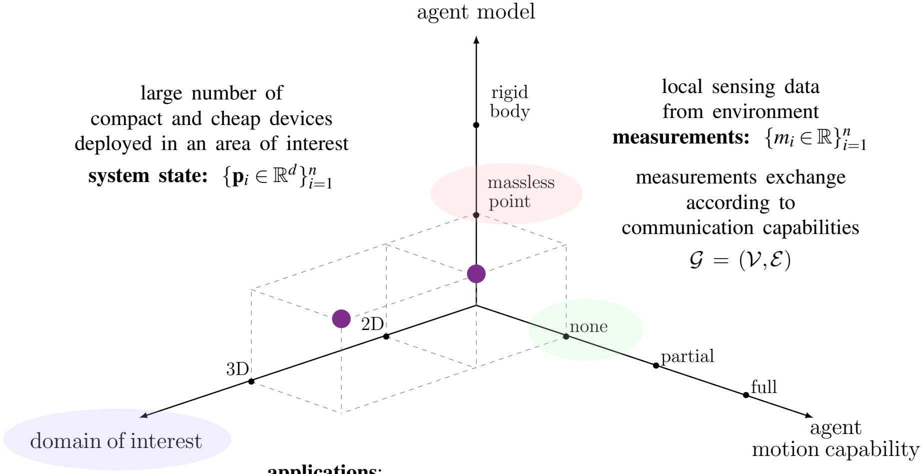

applications:
global monitoring tasks ranging
from factory automation to ambient assisted living
(*event and fault detection*)

Clustering Task

network decomposition + data clustering

C1. connectivity
C2. measurement similarity
C3. maximality

A. Cenedese, M. Luvisotto, **G. Michieletto**. *Distributed Clustering Strategies in Industrial Wireless Sensor Networks*. IEEE Transactions on Industrial Informatics, 13(1):228–237, 2017.
G. Bianchin, A. Cenedese, M. Luvisotto, **G. Michieletto**. *Distributed Fault Detection in Sensor Networks via Clustering and Consensus*. IEEE 54th Annual Conference on Decision and Control (CDC), pages 3828–3833, 2015.

Clustering Task

network decomposition + data clustering

C1. connectivity
C2. measurement similarity
C3. maximality

Centralized Clustering Algorithm (CCA) | Decentralized Clustering Algorithm (DCA)

A. Cenedese, M. Luvisotto, **G. Michieletto**. *Distributed Clustering Strategies in Industrial Wireless Sensor Networks*. IEEE Transactions on Industrial Informatics, 13(1):228–237, 2017.
G. Bianchin, A. Cenedese, M. Luvisotto, **G. Michieletto**. *Distributed Fault Detection in Sensor Networks via Clustering and Consensus*. IEEE 54th Annual Conference on Decision and Control (CDC), pages 3828–3833, 2015.

Clustering Task

network decomposition + *data clustering*

C1. connectivity
C2. measurement similarity
C3. maximality

Centralized Clustering Algorithm (CCA)	Decentralized Clustering Algorithm (DCA)

- input : $\mathbf{m}$, $\mathbf{A}$, b (*clustering bound*)
- output : $\{\mathcal{C}(v_i)\}_{i=1}^n$
- two-steps iterative procedure
  1. inclusion of nodes in clusters
  2. update of bounds
- complexity $O(n^3)$

A. Cenedese, M. Luvisotto, **G. Michieletto**. *Distributed Clustering Strategies in Industrial Wireless Sensor Networks*. IEEE Transactions on Industrial Informatics, 13(1):228–237, 2017.

G. Bianchin, A. Cenedese, M. Luvisotto, **G. Michieletto**. *Distributed Fault Detection in Sensor Networks via Clustering and Consensus*. IEEE 54th Annual Conference on Decision and Control (CDC), pages 3828–3833, 2015.

Clustering Task

network decomposition + *data clustering*

C1. connectivity
C2. measurement similarity
C3. maximality

Centralized Clustering Algorithm (CCA)

- input : $\mathbf{m}$, $\mathbf{A}$, b (*clustering bound*)
- output : $\{\mathcal{C}(v_i)\}_{i=1}^n$
- two-steps iterative procedure
  1. inclusion of nodes in clusters
  2. update of bounds
- complexity $O(n^3)$

Decentralized Clustering Algorithm (DCA)

- input : m_i, $\mathcal{N}_i$, b (*clustering bound*)
- output : c_i
- two-steps iterative procedure
  1. inclusion of neighbors in clusters
  2. update of bounds
- same solution of CCA

A. Cenedese, M. Luvisotto, **G. Michieletto**. *Distributed Clustering Strategies in Industrial Wireless Sensor Networks*. IEEE Transactions on Industrial Informatics, 13(1):228–237, 2017.
G. Bianchin, A. Cenedese, M. Luvisotto, **G. Michieletto**. *Distributed Fault Detection in Sensor Networks via Clustering and Consensus*. IEEE 54th Annual Conference on Decision and Control (CDC), pages 3828–3833, 2015.

Clustering Task

network decomposition + data clustering

C1. connectivity

C2. measurement similarity

C3. maximality

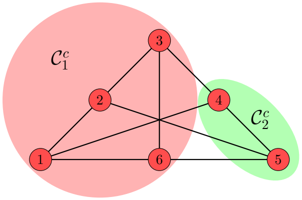

$\mathbf{m} = [10\ 12\ 13\ 20\ 22\ 11]$, $b = 2$

Centralized Clustering Algorithm (CCA)

- input : $\mathbf{m}$, $\mathbf{A}$, b (*clustering bound*)
- output : $\{\mathcal{C}(v_i)\}_{i=1}^n$
- two-steps iterative procedure
  1. inclusion of nodes in clusters
  2. update of bounds
- complexity $O(n^3)$

Decentralized Clustering Algorithm (DCA)

- input : m_i, $\mathcal{N}_i$, b (*clustering bound*)
- output : c_i
- two-steps iterative procedure
  1. inclusion of neighbors in clusters
  2. update of bounds
- same solution of CCA

A. Cenedese, M. Luvisotto, **G. Michieletto**. *Distributed Clustering Strategies in Industrial Wireless Sensor Networks*. IEEE Transactions on Industrial Informatics, 13(1):228–237, 2017.

G. Bianchin, A. Cenedese, M. Luvisotto, **G. Michieletto**. *Distributed Fault Detection in Sensor Networks via Clustering and Consensus*. IEEE 54th Annual Conference on Decision and Control (CDC), pages 3828–3833, 2015.

Application to Industrial Scenario

- environmental sensing

(temperature monitoring in a structured indoor area)

- factory process monitoring

(measurement fault, timing mismatch, communication fault)

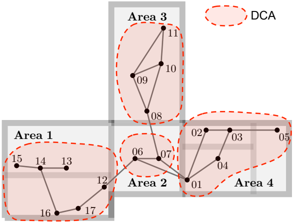

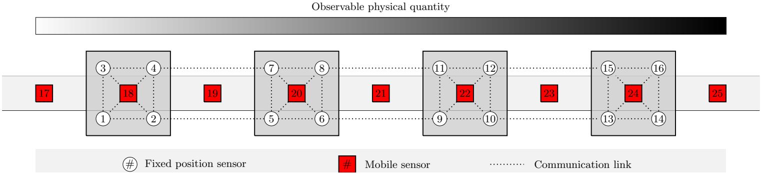

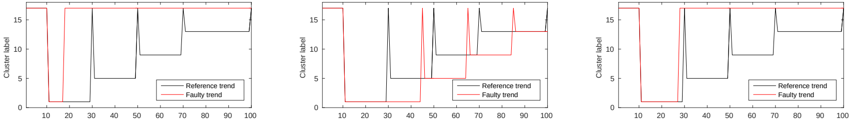

A. Cenedese, M. Luvisotto, **G. Michieletto**. *Distributed Clustering Strategies in Industrial Wireless Sensor Networks*. IEEE Transactions on Industrial Informatics, 13(1): 228–237, 2017.

G. Bianchin, A. Cenedese, M. Luvisotto, **G. Michieletto**. *Distributed Fault Detection in Sensor Networks via Clustering and Consensus*. IEEE 54th Annual Conference on Decision and Control (CDC), pages 3828–3833, 2015.

VSNs - Visual Sensor Networks

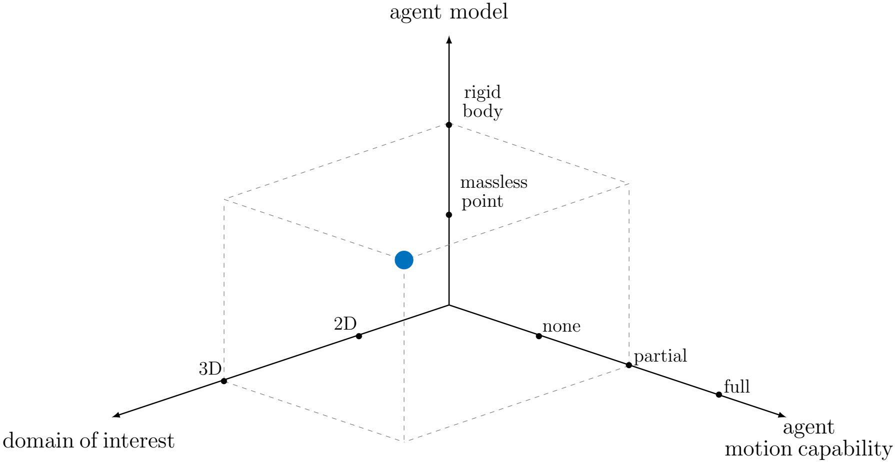

VSNs - Visual Sensor Networks

collection of spatially distributed
smart camera-devices

system state: $\{\mathbf{p}_i, \mathbf{R}_i \in \mathbb{R}^3 \times SO(3)\}_{i=1}^n$

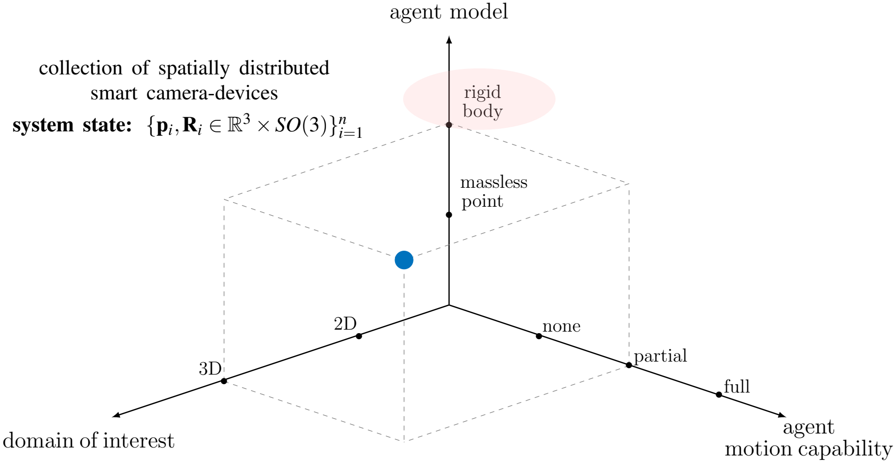

VSNs - Visual Sensor Networks

collection of spatially distributed
smart camera-devices

system state: $\{\mathbf{p}_i, \mathbf{R}_i \in \mathbb{R}^3 \times SO(3)\}_{i=1}^{n}$

image acquisition
varying the orientation

variable attitude: $\{\mathbf{R}_i\}_{i=1}^{n}$

scene data exchange
if overlapping FoVs

$\mathcal{G} = (\mathcal{V}, \mathcal{E})$

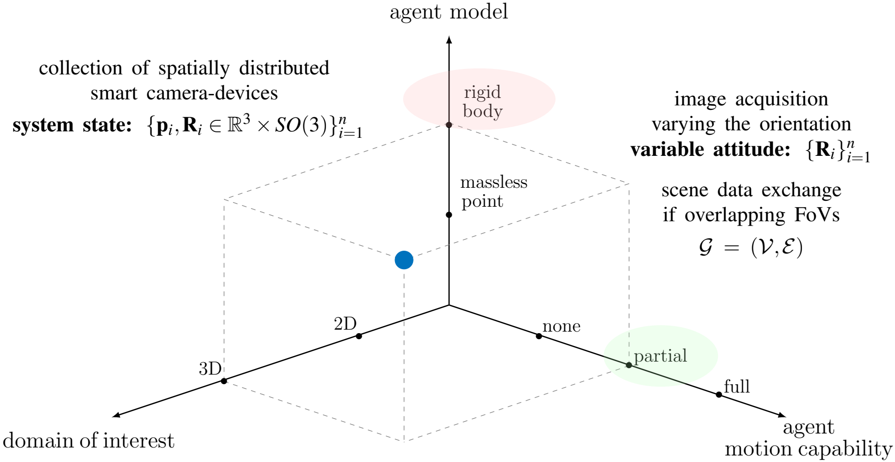

VSNs - Visual Sensor Networks

collection of spatially distributed
smart camera-devices

system state: $\{\mathbf{p}_i, \mathbf{R}_i \in \mathbb{R}^3 \times SO(3)\}_{i=1}^n$

image acquisition
varying the orientation

variable attitude: $\{\mathbf{R}_i\}_{i=1}^n$

scene data exchange
if overlapping FoVs

$\mathcal{G} = (\mathcal{V}, \mathcal{E})$

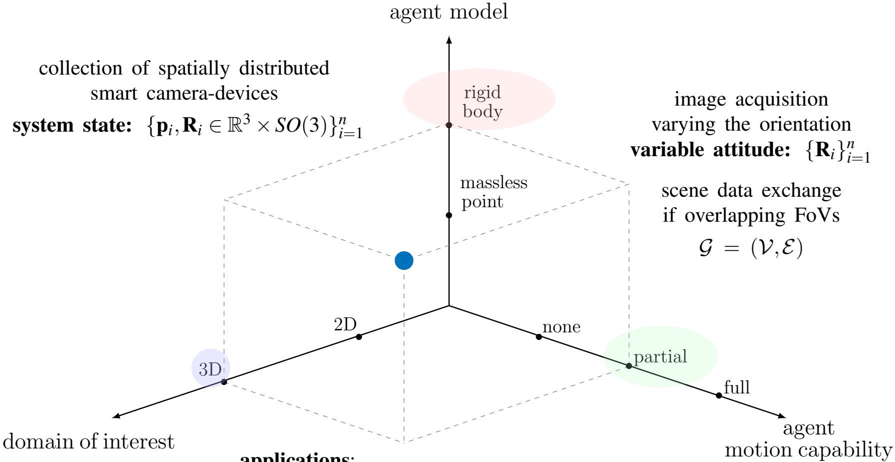

applications:
industrial or civil areas surveillance,
perimeter patrolling and control,
intrusion detection and tracking

→ prerequisite: *calibrated systems*

Attitude Estimation

reference interpretation (body to world frame)

- relative orientation
  $${}^{i}\mathbf{R}_j = \mathbf{R}_i^{-1} \circ \mathbf{R}_j = \mathbf{R}_i^{\top}\mathbf{R}_j$$
- absolute orientation
  $$\mathbf{R}_j = \mathbf{R}_i \circ {}^{i}\mathbf{R}_j = \mathbf{R}_i\,{}^{i}\mathbf{R}_j$$

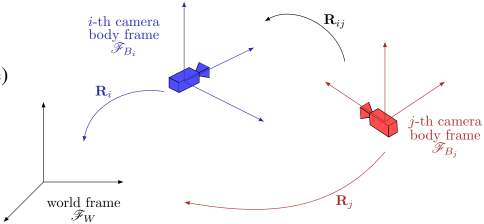

G. Michieletto, S. Milani, A. Cenedese, G. Baggio. *Distributed Camera Calibration for Ad-Hoc Camera Networks via Edge Pruning and Graph Trasversal Initialization.* IEEE 43th International Conference on Acoustic, Speech, and Signal Processing (ICASSP), accepted.

Attitude Estimation

reference interpretation (body to world frame)

- relative orientation
  $${}^{i}\mathbf{R}_j = \mathbf{R}_i^{-1} \circ \mathbf{R}_j = \mathbf{R}_i^{\top}\mathbf{R}_j$$
- absolute orientation
  $$\mathbf{R}_j = \mathbf{R}_i \circ {}^{i}\mathbf{R}_j = \mathbf{R}_i\, {}^{i}\mathbf{R}_j$$

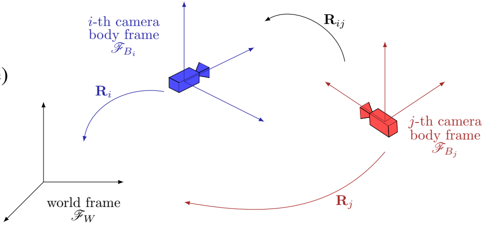

$$J = \sum_{v_i \in \mathcal{V}} \sum_{v_j \in \mathcal{N}_i} \left(\frac{1}{2} d^2_{SO(3)}({}^{i}\widehat{\mathbf{R}}_j, {}^{i}\widetilde{\mathbf{R}}_j) \right) = \sum_{v_i \in \mathcal{V}} \sum_{v_j \in \mathcal{N}_i} \left(\frac{1}{2} d^2_{SO(3)}(\widehat{\mathbf{R}}_i^{\top} \widehat{\mathbf{R}}_j, {}^{i}\widetilde{\mathbf{R}}_j) \right)$$

iterative minimization on $SO(3)$ via Riemannian gradient descent [Tron-Vidal 2014]

G. Michieletto, S. Milani, A. Cenedese, G. Baggio. *Distributed Camera Calibration for Ad-Hoc Camera Networks via Edge Pruning and Graph Trasversal Initialization.* IEEE 43th International Conference on Acoustic, Speech, and Signal Processing (ICASSP), accepted.

Attitude Estimation

reference interpretation (body to world frame)

- relative orientation

$$ {}^{i}\mathbf{R}_j = \mathbf{R}_i^{-1} \circ \mathbf{R}_j = \mathbf{R}_i^{\top} \mathbf{R}_j $$

- absolute orientation

$$ \mathbf{R}_j = \mathbf{R}_i \circ {}^{i}\mathbf{R}_j = \mathbf{R}_i \, {}^{i}\mathbf{R}_j $$

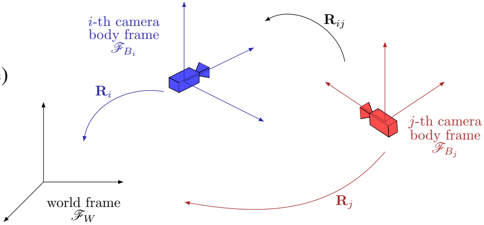

$$ J = \sum_{v_i \in \mathcal{V}} \sum_{v_j \in \mathcal{N}_i} \left(\frac{1}{2} d^2_{SO(3)} ({}^{i}\widehat{\mathbf{R}}_j, {}^{i}\widetilde{\mathbf{R}}_j) \right) = \sum_{v_i \in \mathcal{V}} \sum_{v_j \in \mathcal{N}_i} \left(\frac{1}{2} d^2_{SO(3)} (\widehat{\mathbf{R}}_i^{\top} \widehat{\mathbf{R}}_j, {}^{i}\widetilde{\mathbf{R}}_j) \right) $$

non-convex

iterative minimization on $SO(3)$ via Riemannian gradient descent [Tron-Vidal 2014]

G. Michieletto, S. Milani, A. Cenedese, G. Baggio. *Distributed Camera Calibration for Ad-Hoc Camera Networks via Edge Pruning and Graph Trasversal Initialization.* IEEE 43th International Conference on Acoustic, Speech, and Signal Processing (ICASSP), accepted.

Attitude Estimation

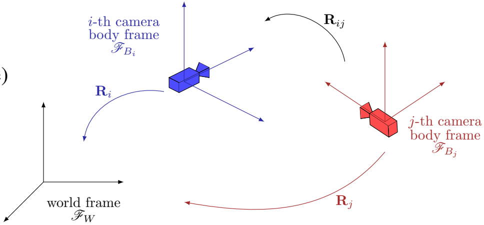

reference interpretation (body to world frame)

- relative orientation

$$ {}^i\mathbf{R}_j = \mathbf{R}_i^{-1} \circ \mathbf{R}_j = \mathbf{R}_i^\top \mathbf{R}_j $$

- absolute orientation

$$ \mathbf{R}_j = \mathbf{R}_i \circ {}^i\mathbf{R}_j = \mathbf{R}_i \, {}^i\mathbf{R}_j $$

$$ J = \sum_{v_i \in \mathcal{V}} \sum_{v_j \in \mathcal{N}_i} \left(\frac{1}{2} d^2_{SO(3)} ({}^i\widehat{\mathbf{R}}_j, {}^i\widetilde{\mathbf{R}}_j) \right) = \sum_{v_i \in \mathcal{V}} \sum_{v_j \in \mathcal{N}_i} \left(\frac{1}{2} d^2_{SO(3)} (\widehat{\mathbf{R}}_i^\top \widehat{\mathbf{R}}_j, {}^i\widetilde{\mathbf{R}}_j) \right) $$

non-convex

iterative minimization on $SO(3)$ via Riemannian gradient descent [Tron-Vidal 2014]

Graph-Based Ad-Hoc Initialization Methods

Single Spanning Tree (SST) + Multi Paths (MP)
averaged Single Spanning Tree (aSST)
averaged Multi Paths (aMP)

G. Michieletto, S. Milani, A. Cenedese, G. Baggio. *Distributed Camera Calibration for Ad-Hoc Camera Networks via Edge Pruning and Graph Trasversal Initialization.* IEEE 43th International Conference on Acoustic, Speech, and Signal Processing (ICASSP), accepted.

Application Scenario

- ▲ a priori information explotation (topology+measurements)
- ▲ robustness to noise
- ▼ computational burden

	SST	aSST	MP	aMP
$e_R(0)$	0.145	0.072	0.108	0.065
$e_R(t_{max})$	0.097	0.064	0.090	0.065

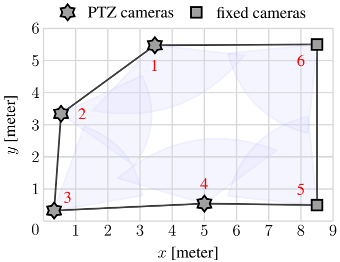

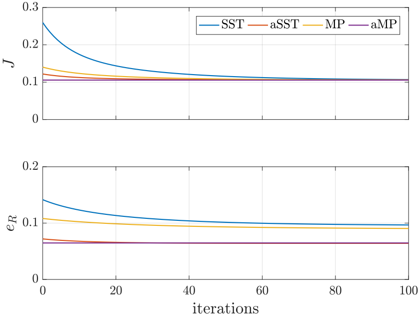

G. Michieletto, S. Milani, A. Cenedese, G. Baggio. *Distributed Camera Calibration for Ad-Hoc Camera Networks via Edge Pruning and Graph Trasversal Initialization.* IEEE 43th International Conference on Acoustic, Speech, and Signal Processing (ICASSP), accepted.

VSNs - Visual Sensor Networks

Pan-Only cameras

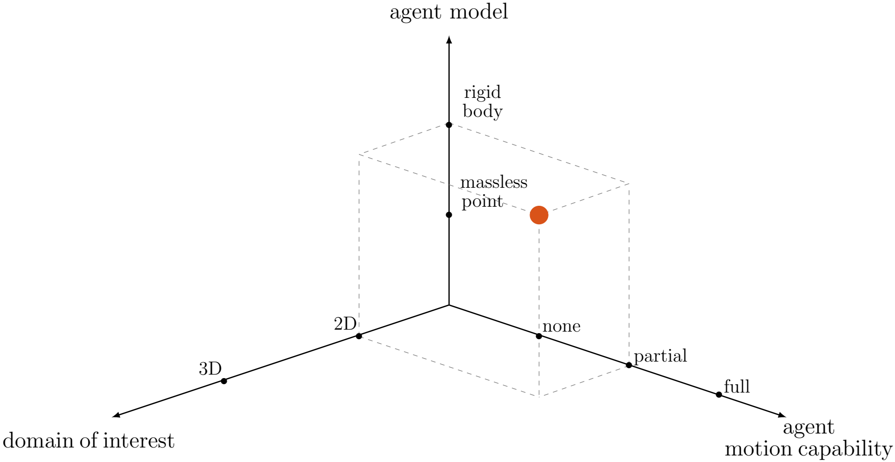

VSNs - Visual Sensor Networks

Pan-Only cameras

collection of spatially distributed
smart (pan-only) camera-devices

system state: $\{\mathbf{p}_i, \mathbf{R}_i \in \mathbb{R}^2 \times SO(2)\}_{i=1}^n$
$\cong \{\mathbf{p}_i, \psi_i \in \mathbb{R}^2 \times \mathbb{S}^1\}_{i=1}^n$

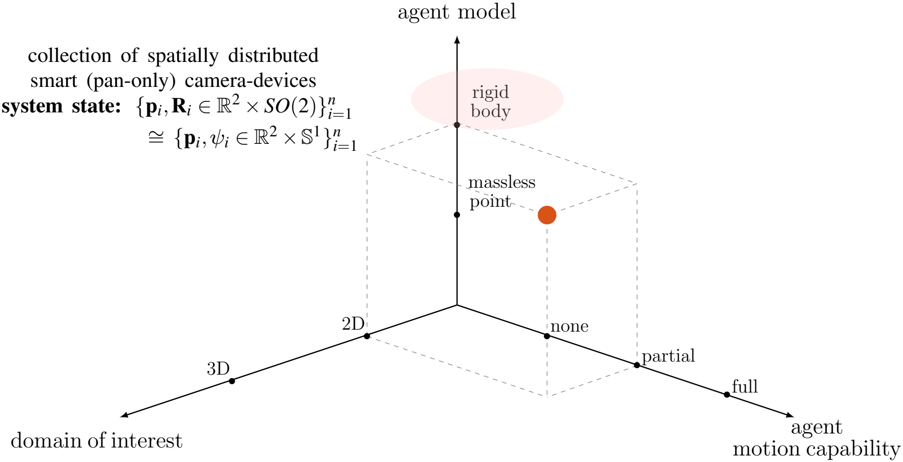

VSNs - Visual Sensor Networks

Pan-Only cameras

collection of spatially distributed
smart (pan-only) camera-devices
system state: $\{\mathbf{p}_i, \mathbf{R}_i \in \mathbb{R}^2 \times SO(2)\}_{i=1}^n$
$\cong \{\mathbf{p}_i, \psi_i \in \mathbb{R}^2 \times \mathbb{S}^1\}_{i=1}^n$

image acquisition through
rotation around a single axis
variable pan angle: $\{\psi_i\}_{i=1}^n$

scene data exchange
if overlapping FoVs
$\mathcal{G} = (\mathcal{V}, \mathcal{E})$

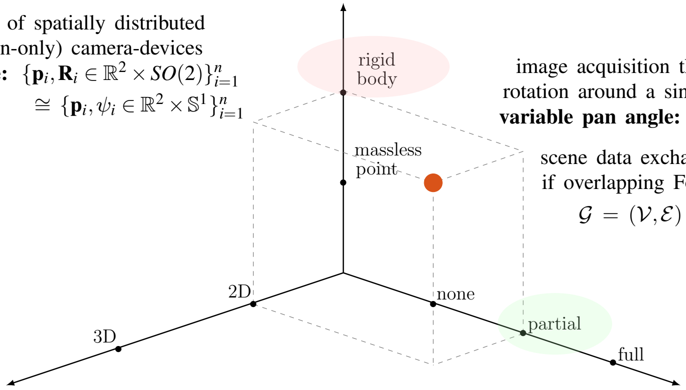

VSNs - Visual Sensor Networks

Pan-Only cameras

collection of spatially distributed
smart (pan-only) camera-devices

system state: $\{\mathbf{p}_i, \mathbf{R}_i \in \mathbb{R}^2 \times SO(2)\}_{i=1}^n$
$\cong \{\mathbf{p}_i, \psi_i \in \mathbb{R}^2 \times \mathbb{S}^1\}_{i=1}^n$

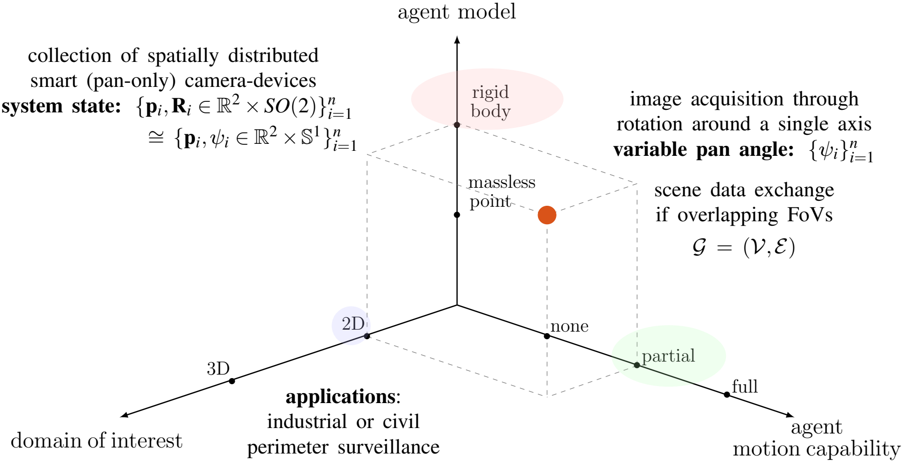

image acquisition through
rotation around a single axis
variable pan angle: $\{\psi_i\}_{i=1}^n$

scene data exchange
if overlapping FoVs
$\mathcal{G} = (\mathcal{V}, \mathcal{E})$

applications:
industrial or civil
perimeter surveillance

$\rightarrow$ prerequisite: *calibrated systems*

Attitude Estimation

2D scenario:
from rotation synchronization
to angular synchronization

$$J = \sum_{v_i \in \mathcal{V}} \sum_{v_j \in \mathcal{N}_i} \left(\frac{1}{2} (\hat{\psi}_i - \hat{\psi}_j - {}^i\tilde{\psi}_j)^2 \right)$$

M. Fabris, **G. Michieletto** and A. Cenedese. *Distributed Rotation Synchronization in SO(2) for a Camera Network.* IEEE 57th Conference on Decision and Control (CDC), submitted.

Attitude Estimation

2D scenario:
from rotation synchronization
to angular synchronization

$$J = \sum_{v_i \in \mathcal{V}} \sum_{v_j \in \mathcal{N}_i} \left(\frac{1}{2} (\hat{\psi}_i - \hat{\psi}_j - {}^i\tilde{\psi}_j)^2 \right)$$

convex

M. Fabris, **G. Michieletto** and A. Cenedese. *Distributed Rotation Synchronization in SO(2) for a Camera Network.* IEEE 57th Conference on Decision and Control (CDC), submitted.

Attitude Estimation

2D scenario:
from rotation synchronization
to angular synchronization

$$J = \sum_{v_i \in \mathcal{V}} \sum_{v_j \in \mathcal{N}_i} \left(\frac{1}{2} (\hat{\psi}_i - \hat{\psi}_j - {}^i\tilde{\psi}_j)^2 \right)$$

convex

State-space model 1	State-space model 2

M. Fabris, **G. Michieletto** and A. Cenedese. *Distributed Rotation Synchronization in SO(2) for a Camera Network.* IEEE 57th Conference on Decision and Control (CDC), submitted.

Attitude Estimation

2D scenario:
from rotation synchronization
to angular synchronization

$$J = \sum_{v_i \in \mathcal{V}} \sum_{v_j \in \mathcal{N}_i} \left(\frac{1}{2} (\hat{\psi}_i - \hat{\psi}_j -^i \tilde{\psi}_j)^2 \right)$$

convex

State-space model 1	State-space model 2

$$\widehat{\boldsymbol{\psi}}(t+1) = \mathbf{F}\widehat{\boldsymbol{\psi}}(t) + \mathbf{u} \qquad \mathbf{F} = \mathbf{D}^{-1}\mathbf{A}$$

$$\mathbf{u} = \frac{1}{2}\mathbf{D}^{-1}\widetilde{\boldsymbol{\psi}}$$

$$\Lambda_{\mathbf{F}} = \{\lambda_i \in [-1, 1], i = 0 \dots N-1\}$$

M. Fabris, **G. Michieletto** and A. Cenedese. *Distributed Rotation Synchronization in SO(2) for a Camera Network.* IEEE 57th Conference on Decision and Control (CDC), submitted.

Attitude Estimation

2D scenario:
from rotation synchronization
to angular synchronization

$$J = \sum_{v_i \in \mathcal{V}} \sum_{v_j \in \mathcal{N}_i} \left(\frac{1}{2} (\hat{\psi}_i - \hat{\psi}_j - {}^i \tilde{\psi}_j)^2 \right)$$

convex

State-space model 1	State-space model 2

$$\widehat{\boldsymbol{\psi}}(t+1) = \mathbf{F}\widehat{\boldsymbol{\psi}}(t) + \mathbf{u} \qquad \mathbf{F} = \mathbf{D}^{-1}\mathbf{A}$$

$$\mathbf{u} = \frac{1}{2}\mathbf{D}^{-1}\widetilde{\boldsymbol{\psi}}$$

$$\Lambda_{\mathbf{F}} = \{\lambda_i \in [-1, 1], i = 0 \dots N-1\}$$

- convergence dependence on network topology: oscillations $\leftrightarrow$ bipartite graph
- edge selection to avoid oscillations

M. Fabris, **G. Michieletto** and A. Cenedese. *Distributed Rotation Synchronization in SO(2) for a Camera Network.* IEEE 57th Conference on Decision and Control (CDC), submitted.

Attitude Estimation

2D scenario:
from rotation synchronization
to angular synchronization

$$J = \sum_{v_i \in \mathcal{V}} \sum_{v_j \in \mathcal{N}_i} \left(\frac{1}{2} (\hat{\psi}_i - \hat{\psi}_j - {}^i\tilde{\psi}_j)^2 \right)$$

convex

State-space model 1	State-space model 2

State-space model 1

$$\widehat{\boldsymbol{\psi}}(t+1) = \mathbf{F}\widehat{\boldsymbol{\psi}}(t) + \mathbf{u} \qquad \mathbf{F} = \mathbf{D}^{-1}\mathbf{A}$$

$$\mathbf{u} = \frac{1}{2}\mathbf{D}^{-1}\widetilde{\boldsymbol{\psi}}$$

$$\Lambda_{\mathbf{F}} = \{\lambda_i \in [-1, 1], i = 0 \ldots N-1\}$$

- convergence dependence on network topology: oscillations $\leftrightarrow$ bipartite graph
- edge selection to avoid oscillations

State-space model 2

$$\widehat{\boldsymbol{\psi}}(k+1) = \eta\widehat{\boldsymbol{\psi}}(k) + (1-\eta)\left(\mathbf{F}\widehat{\boldsymbol{\psi}}(k) + \mathbf{u}\right)$$
$$= \mathbf{F}'(\eta)\widehat{\boldsymbol{\psi}}(k) + (1-\eta)\mathbf{u} \qquad \eta \in (0,1)$$

$$\Lambda_{\mathbf{F}'} = \{\lambda_i \in [-1+2\eta, 1], i = 0 \ldots N-1\}$$

M. Fabris, **G. Michieletto** and A. Cenedese. *Distributed Rotation Synchronization in SO(2) for a Camera Network.* IEEE 57th Conference on Decision and Control (CDC), submitted.

Attitude Estimation

2D scenario:
from rotation synchronization
to angular synchronization

$$J = \sum_{v_i \in \mathcal{V}} \sum_{v_j \in \mathcal{N}_i} \left(\tfrac{1}{2} (\hat{\psi}_i - \hat{\psi}_j - {}^i\tilde{\psi}_j)^2 \right)$$

convex

State-space model 1	State-space model 2

State-space model 1

$$\widehat{\boldsymbol{\psi}}(t+1) = \mathbf{F}\widehat{\boldsymbol{\psi}}(t) + \mathbf{u} \qquad \mathbf{F} = \mathbf{D}^{-1}\mathbf{A}$$

$$\mathbf{u} = \frac{1}{2}\mathbf{D}^{-1}\widetilde{\boldsymbol{\psi}}$$

$$\Lambda_{\mathbf{F}} = \{\lambda_i \in [-1, 1], i = 0 \dots N-1\}$$

- convergence dependence on network topology: oscillations $\leftrightarrow$ bipartite graph
- edge selection to avoid oscillations

State-space model 2

$$\begin{aligned}\widehat{\boldsymbol{\psi}}(k+1) &= \eta\widehat{\boldsymbol{\psi}}(k) + (1-\eta)\left(\mathbf{F}\widehat{\boldsymbol{\psi}}(k) + \mathbf{u}\right) \\ &= \mathbf{F}'(\eta)\widehat{\boldsymbol{\psi}}(k) + (1-\eta)\mathbf{u} \quad \eta \in (0,1)\end{aligned}$$

$$\Lambda_{\mathbf{F}'} = \{\lambda_i \in [-1+2\eta, 1], i = 0 \dots N-1\}$$

- convergence dependence on control parameter η: self-loops introduction
- η tuning for optimal performance

M. Fabris, **G. Michieletto** and A. Cenedese. *Distributed Rotation Synchronization in SO(2) for a Camera Network.* IEEE 57th Conference on Decision and Control (CDC), submitted.

Application to Ring Camera Network

6 cameras
(bipartite graph)

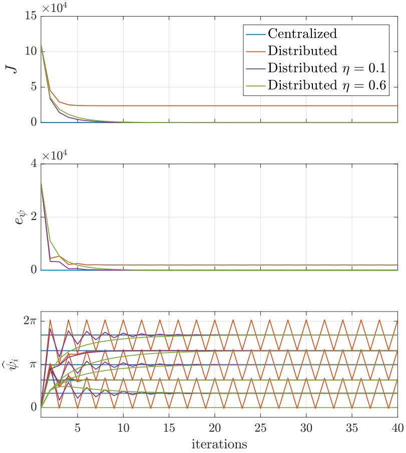

7 cameras
(non-bipartite graph)

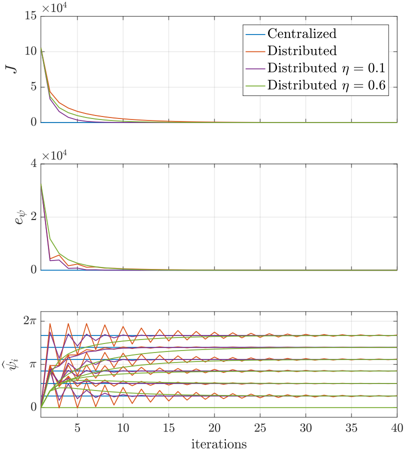

M. Fabris, **G. Michieletto** and A. Cenedese. *Distributed Rotation Synchronization in SO(2) for a Camera Network.* IEEE 57th Conference on Decision and Control (CDC), submitted.

Perimeter Patrolling

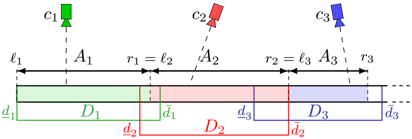

minimization of the maximum time interval between two consecutive visits of the same point

$$\{A_i^*\}_{i=1}^n = min\, max_i \{T_{lag}^*(A_i)\}$$
$$\text{s.t.} \quad A_i \subseteq D_i$$
$$\cup_i^n A_i = \mathcal{L}$$

G. Belgioioso, A. Cenedese, **G. Michieletto**. *Distributed partitioning strategies with visual optimization for camera network perimeter patrolling.* IEEE 55th Conference on Decision and Control (CDC), pp. 5912-5917, 2016.

Perimeter Patrolling

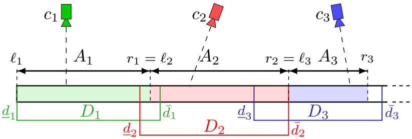

minimization of the maximum time interval between two consecutive visits of the same point

$$
\begin{aligned}
\{A_i^*\}_{i=1}^n = min\, max_i \{T_{lag}^*(A_i)\} \\
\text{s.t.} \quad A_i \subseteq D_i \\
\cup_i^n A_i = \mathcal{L}
\end{aligned}
$$

distributed symmetric-gossip perimeter partitioning algorithm (s-PAC)

G. Belgioioso, A. Cenedese, **G. Michieletto**. *Distributed partitioning strategies with visual optimization for camera network perimeter patrolling.* IEEE 55th Conference on Decision and Control (CDC), pp. 5912-5917, 2016.

Perimeter Patrolling

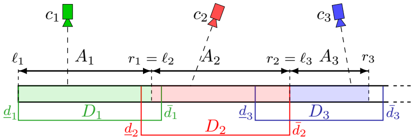

minimization of the maximum time interval between two consecutive visits of the same point

$$
\begin{aligned}
\{A_i^*\}_{i=1}^n = min\, max_i \{T^*_{lag}(A_i)\} \\
\text{s.t.} \quad A_i \subseteq D_i \\
\cup_i^n A_i = \mathcal{L}
\end{aligned}
$$

distributed symmetric-gossip perimeter partitioning algorithm (s-PAC)

- from segment to perimeter partitioning

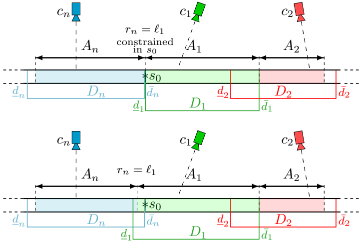

G. Belgioioso, A. Cenedese, **G. Michieletto**. *Distributed partitioning strategies with visual optimization for camera network perimeter patrolling.* IEEE 55th Conference on Decision and Control (CDC), pp. 5912-5917, 2016.

Perimeter Patrolling

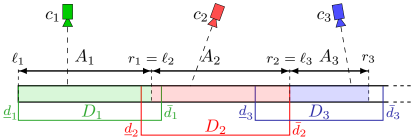

minimization of the maximum time interval between two consecutive visits of the same point

$$\{A_i^*\}_{i=1}^n = min\, max_i \{T^*_{lag}(A_i)\}$$
$$\text{s.t.} \quad A_i \subseteq D_i$$
$$\cup_i^n A_i = \mathcal{L}$$

distributed symmetric-gossip perimeter partitioning algorithm (s-PAC)

- from segment to perimeter partitioning

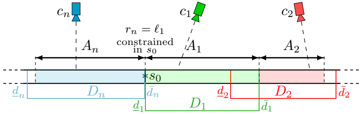

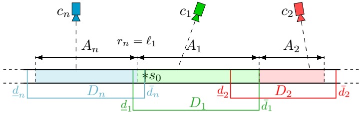

- vision quality centering criterion (penalty function)

$$H_i : x \in D_i \ \rightarrow |\varphi_i| \in [0, \pi/2)$$
$$q(A_i) = \int_{A_i} H(z_i) dz_i$$

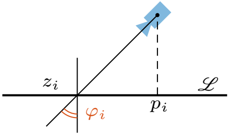

G. Belgioioso, A. Cenedese, **G. Michieletto**. *Distributed partitioning strategies with visual optimization for camera network perimeter patrolling.* IEEE 55th Conference on Decision and Control (CDC), pp. 5912-5917, 2016.

Application Scenario

- perimeter patritioning according to lag time minimization only
  $\rightarrow$ multiple optimal solutions

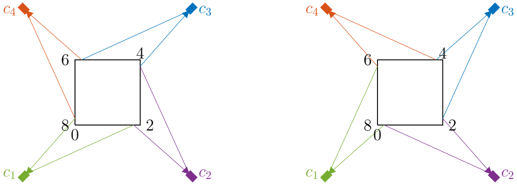

- enhancement of visual quality via introduction of centering criterion

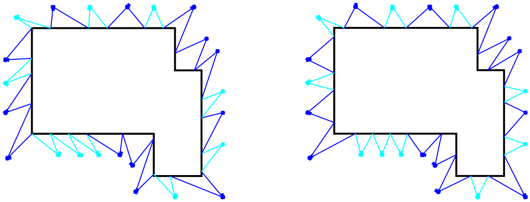

G. Belgioioso, A. Cenedese, **G. Michieletto**. *Distributed partitioning strategies with visual optimization for camera network perimeter patrolling.* IEEE 55th Conference on Decision and Control (CDC), pp. 5912-5917, 2016.

UAVs - Unmanned Aerial Vehicles

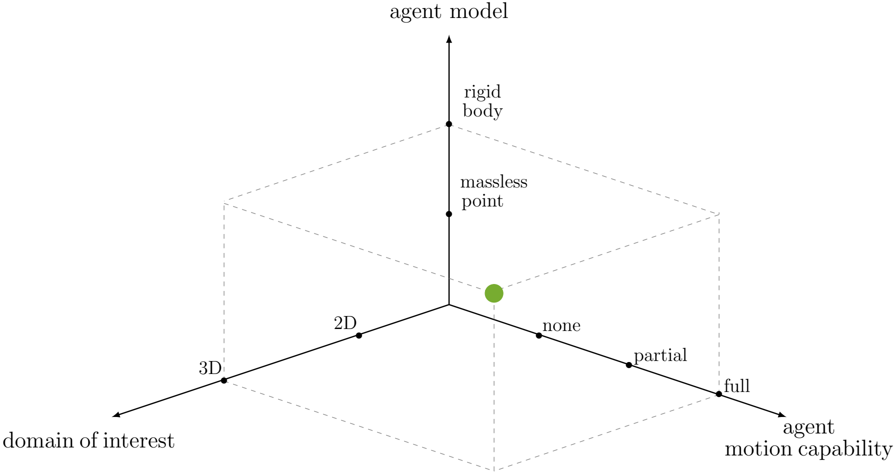

UAVs - Unmanned Aerial Vehicles

swarm of autonomous
multi-rotor aerial vehicles

system state: $\{\mathbf{p}_i, \mathbf{R}_i \in \mathbb{R}^3 \times SO(3)\}_{i=1}^n$

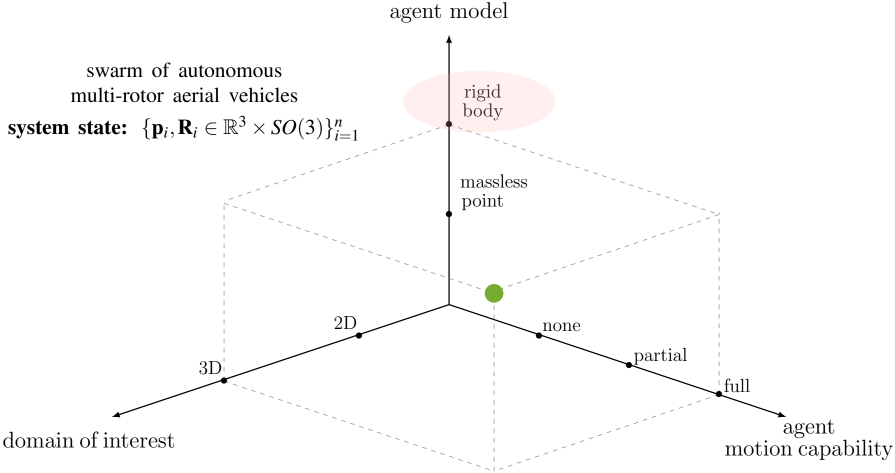

UAVs - Unmanned Aerial Vehicles

swarm of autonomous
multi-rotor aerial vehicles

system state: $\{\mathbf{p}_i, \mathbf{R}_i \in \mathbb{R}^3 \times SO(3)\}_{i=1}^{n}$

six DoFs
variable poses: $\{\mathbf{p}_i, \mathbf{R}_i\}$

state information
exchange
$\mathcal{G} = (\mathcal{V}, \mathcal{E})$

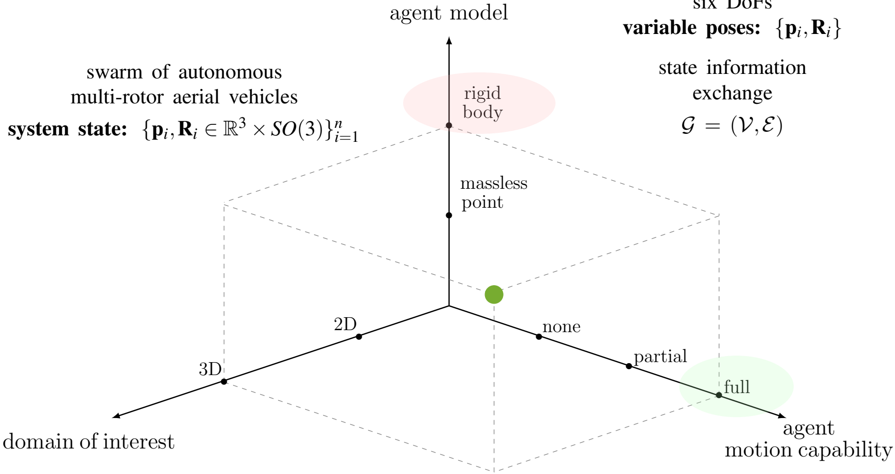

UAVs - Unmanned Aerial Vehicles

swarm of autonomous
multi-rotor aerial vehicles

system state: $\{\mathbf{p}_i, \mathbf{R}_i \in \mathbb{R}^3 \times SO(3)\}_{i=1}^n$

six DoFs
variable poses: $\{\mathbf{p}_i, \mathbf{R}_i\}$

state information
exchange
$\mathcal{G} = (\mathcal{V}, \mathcal{E})$

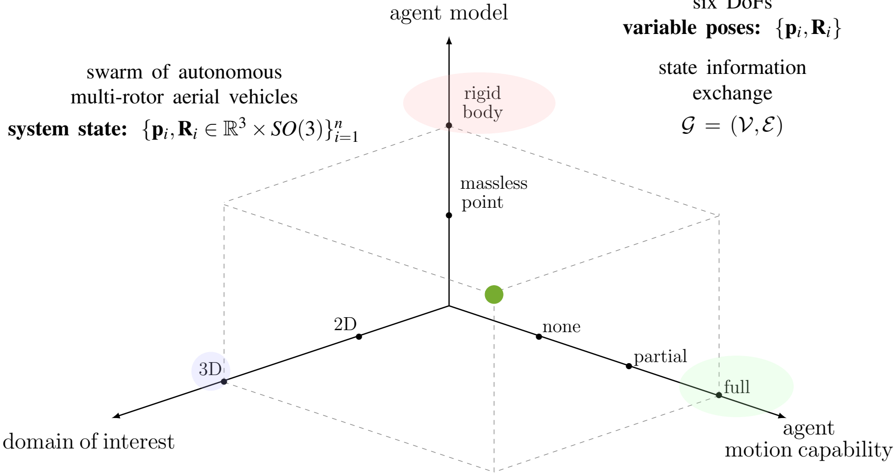

applications:
exploration and mapping, grasping and transportation,
monitoring and surveillance,
cooperative manipulation and human and environment interaction

(*real-world deployment*)

Actuation Properties Analysis

UAV with $n \geq 4$ propellers

$$\mathbf{f}_i = c_{f_i} u_i \mathbf{z}_{P_i} \qquad \mathbf{f}_c = \sum_{i=1}^{n} \mathbf{f}_i = \mathbf{F}\mathbf{u}$$

$$\boldsymbol{\tau}_i^d = c_{\tau_i} u_i \mathbf{z}_{P_i} \qquad \boldsymbol{\tau}_c = \sum_{i=1}^{n} (\boldsymbol{\tau}_i^t + \boldsymbol{\tau}_i^d) = \mathbf{M}\mathbf{u}$$

$$\boldsymbol{\tau}_i^t = c_{f_i} u_i (\mathbf{p}_i \times \mathbf{z}_{P_i}) \qquad \mathbf{F} \in \mathbb{R}^{3\times n}, \mathbf{M} \in \mathbb{R}^{3\times n}$$

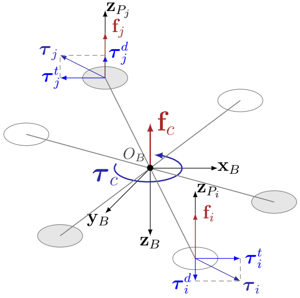

$$m\ddot{\mathbf{p}} = -mg\mathbf{e}_3 + \mathbf{R}\mathbf{f}_c = -mg\mathbf{e}_3 + \mathbf{R}\mathbf{F}\mathbf{u}$$
$$\mathbf{J}\dot{\boldsymbol{\omega}} = -\boldsymbol{\omega} \times \mathbf{J}\boldsymbol{\omega} + \boldsymbol{\tau}_c = -\boldsymbol{\omega} \times \mathbf{J}\boldsymbol{\omega} + \mathbf{M}\mathbf{u}$$

G. Michieletto, M. Ryll and A. Franchi. *Control of statically hoverable multi-rotor aerial vehicles and application to rotor-failure robustness for hexarotors.* IEEE International Conference on Robotics and Automation (ICRA), pp. 2747-2752, 2017.

G. Michieletto, M. Ryll and A. Franchi. *Fundamental Actuation Properties of Multi-rotors: Force-Moment Decoupling and Fail-safe Robustness.* IEEE Transaction on Robotics, accepted.

Actuation Properties Analysis

UAV with $n \geq 4$ propellers

$$\mathbf{f}_i = c_{f_i} u_i \mathbf{z}_{P_i} \qquad \mathbf{f}_c = \sum_{i=1}^n \mathbf{f}_i = \mathbf{F}\mathbf{u}$$

$$\boldsymbol{\tau}_i^d = c_{\tau_i} u_i \mathbf{z}_{P_i} \qquad \boldsymbol{\tau}_c = \sum_{i=1}^n (\boldsymbol{\tau}_i^t + \boldsymbol{\tau}_i^d) = \mathbf{M}\mathbf{u}$$

$$\boldsymbol{\tau}_i^t = c_{f_i} u_i (\mathbf{p}_i \times \mathbf{z}_{P_i}) \qquad \mathbf{F} \in \mathbb{R}^{3\times n}, \mathbf{M} \in \mathbb{R}^{3\times n}$$

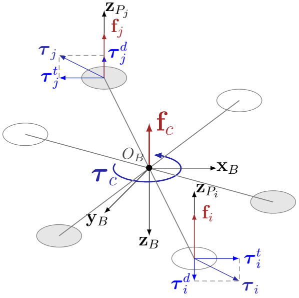

$$m\ddot{\mathbf{p}} = -mg\mathbf{e}_3 + \mathbf{R}\mathbf{f}_c = -mg\mathbf{e}_3 + \mathbf{R}\mathbf{F}\mathbf{u}$$
$$\mathbf{J}\dot{\boldsymbol{\omega}} = -\boldsymbol{\omega} \times \mathbf{J}\boldsymbol{\omega} + \boldsymbol{\tau}_c = -\boldsymbol{\omega} \times \mathbf{J}\boldsymbol{\omega} + \mathbf{M}\mathbf{u}$$

static hovering realizability with unidirectional propeller spin

G. Michieletto, M. Ryll and A. Franchi. *Control of statically hoverable multi-rotor aerial vehicles and application to rotor-failure robustness for hexarotors.* IEEE International Conference on Robotics and Automation (ICRA), pp. 2747-2752, 2017.

G. Michieletto, M. Ryll and A. Franchi. *Fundamental Actuation Properties of Multi-rotors: Force-Moment Decoupling and Fail-safe Robustness.* IEEE Transaction on Robotics, accepted.

Actuation Properties Analysis

UAV with $n \geq 4$ propellers

$$\mathbf{f}_i = c_{f_i} u_i \mathbf{z}_{P_i} \qquad \mathbf{f}_c = \sum_{i=1}^{n} \mathbf{f}_i = \mathbf{F}\mathbf{u}$$

$$\boldsymbol{\tau}_i^d = c_{\tau_i} u_i \mathbf{z}_{P_i} \qquad \boldsymbol{\tau}_c = \sum_{i=1}^{n} (\boldsymbol{\tau}_i^t + \boldsymbol{\tau}_i^d) = \mathbf{M}\mathbf{u}$$

$$\boldsymbol{\tau}_i^t = c_{f_i} u_i (\mathbf{p}_i \times \mathbf{z}_{P_i}) \qquad \mathbf{F} \in \mathbb{R}^{3\times n}, \mathbf{M} \in \mathbb{R}^{3\times n}$$

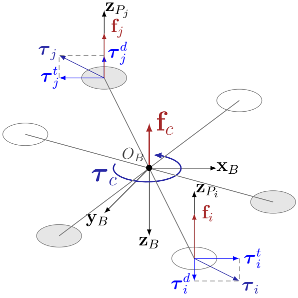

$$\begin{aligned} m\ddot{\mathbf{p}} &= -mg\mathbf{e}_3 + \mathbf{R}\mathbf{f}_c = -mg\mathbf{e}_3 + \mathbf{R}\mathbf{F}\mathbf{u} \\ \mathbf{J}\dot{\boldsymbol{\omega}} &= -\boldsymbol{\omega} \times \mathbf{J}\boldsymbol{\omega} + \boldsymbol{\tau}_c = -\boldsymbol{\omega} \times \mathbf{J}\boldsymbol{\omega} + \mathbf{M}\mathbf{u} \end{aligned}$$

static hovering realizability with unidirectional propeller spin

fly at a constant reference position with constant attitude under the constraint $\mathbf{u} \geq 0$

- $rank(\mathbf{M}) = 3$
- $\exists \mathbf{u} > \mathbf{0}$ s.t. $\mathbf{M}\mathbf{u} = \mathbf{0}$
- $\exists \mathbf{u} \geq \mathbf{0}$ s.t. $\mathbf{M}\mathbf{u} = \mathbf{0}$ and $\mathbf{F}\mathbf{u} \neq \mathbf{0}$

G. Michieletto, M. Ryll and A. Franchi. *Control of statically hoverable multi-rotor aerial vehicles and application to rotor-failure robustness for hexarotors.* IEEE International Conference on Robotics and Automation (ICRA), pp. 2747-2752, 2017.

G. Michieletto, M. Ryll and A. Franchi. *Fundamental Actuation Properties of Multi-rotors: Force-Moment Decoupling and Fail-safe Robustness.* IEEE Transaction on Robotics, accepted.

Fail-Safe Robustness Analysis

fully robustness =

capability of realizing static hover after a propeller loss

G. Michieletto, M. Ryll and A. Franchi. *Control of statically hoverable multi-rotor aerial vehicles and application to rotor-failure robustness for hexarotors.* IEEE International Conference on Robotics and Automation (ICRA), pp. 2747-2752, 2017.

G. Michieletto, M. Ryll and A. Franchi. *Fundamental Actuation Properties of Multi-rotors: Force-Moment Decoupling and Fail-safe Robustness.* IEEE Transaction on Robotics, accepted.

Fail-Safe Robustness Analysis

fully robustness =
capability of realizing static hover after a propeller loss

- ✖ collinear star-shaped hexarotor
- ✓ tilted star-shaped hexarotor
- ✓ collinear Y-shaped hexarotor

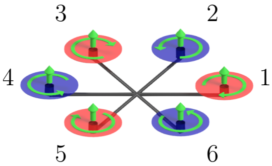

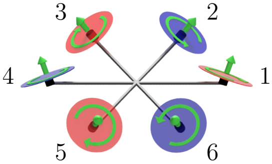

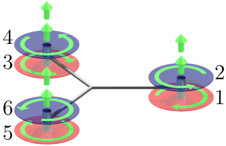

G. Michieletto, M. Ryll and A. Franchi. *Control of statically hoverable multi-rotor aerial vehicles and application to rotor-failure robustness for hexarotors.* IEEE International Conference on Robotics and Automation (ICRA), pp. 2747-2752, 2017.

G. Michieletto, M. Ryll and A. Franchi. *Fundamental Actuation Properties of Multi-rotors: Force-Moment Decoupling and Fail-safe Robustness.* IEEE Transaction on Robotics, accepted.

Fail-Safe Robustness Analysis

fully robustness =
capability of realizing static hover after a propeller loss

- ✖ collinear star-shaped hexarotor
- ✓ tilted star-shaped hexarotor
- ✓ collinear Y-shaped hexarotor

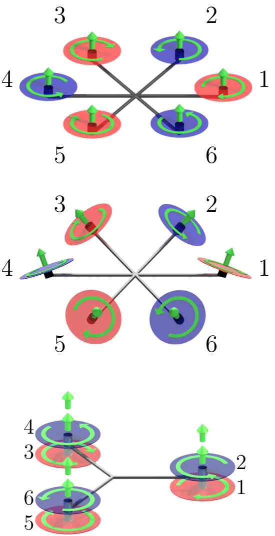

G. **Michieletto**, M. Ryll and A. Franchi. *Control of statically hoverable multi-rotor aerial vehicles and application to rotor-failure robustness for hexarotors.* IEEE International Conference on Robotics and Automation (ICRA), pp. 2747-2752, 2017.

G. **Michieletto**, M. Ryll and A. Franchi. *Fundamental Actuation Properties of Multi-rotors: Force-Moment Decoupling and Fail-safe Robustness.* IEEE Transaction on Robotics, accepted.

Static Hover Control

UAV stabilization: *constant* position and attitude, *zero* linear and angular velocity

G. Michieletto, M. Ryll and A. Franchi. *Control of statically hoverable multi-rotor aerial vehicles and application to rotor-failure robustness for hexarotors.* IEEE International Conference on Robotics and Automation (ICRA), pp. 2747-2752, 2017.

G. Michieletto, A. Cenedese, L. Zaccarian, A. Franchi. *Nonlinear Control of Multi-Rotor Aerial Vehicles Based on the Zero-Moment Direction.* IFAC World Congress 2017, pp. 13686–13691, 2017.

Static Hover Control

UAV stabilization: *constant* position and attitude, *zero* linear and angular velocity

cascaded zero-moment direction based controller

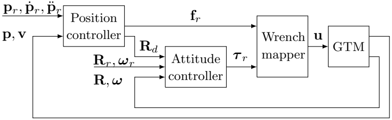

- ► rotation matrix
- ▼ **no** convergence proof
- ▲ simulative results
- ▲ experimental results

G. Michieletto, M. Ryll and A. Franchi. *Control of statically hoverable multi-rotor aerial vehicles and application to rotor-failure robustness for hexarotors.* IEEE International Conference on Robotics and Automation (ICRA), pp. 2747-2752, 2017.

G. Michieletto, A. Cenedese, L. Zaccarian, A. Franchi. *Nonlinear Control of Multi-Rotor Aerial Vehicles Based on the Zero-Moment Direction.* IFAC World Congress 2017, pp. 13686–13691, 2017.

Static Hover Control

UAV stabilization: *constant* position and attitude, *zero* linear and angular velocity

cascaded zero-moment direction based controller

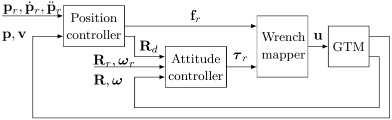

- ▶ rotation matrix
- ▼ **no** convergence proof
- ▲ simulative results
- ▲ experimental results

nonlinear zero-moment direction based controller

- ▶ unit quaternion
- ▲ convergence proof
- ▲ simulative results
- ▼ **no** experimental results

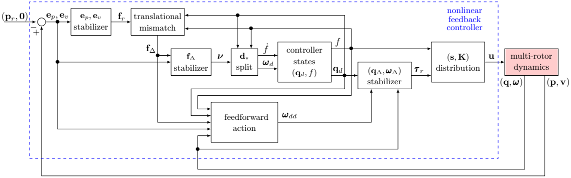

G. Michieletto, M. Ryll and A. Franchi. *Control of statically hoverable multi-rotor aerial vehicles and application to rotor-failure robustness for hexarotors.* IEEE International Conference on Robotics and Automation (ICRA), pp. 2747-2752, 2017.

G. Michieletto, A. Cenedese, L. Zaccarian, A. Franchi. *Nonlinear Control of Multi-Rotor Aerial Vehicles Based on the Zero-Moment Direction.* IFAC World Congress 2017, pp. 13686–13691, 2017.

Simulative Results

failed collinear Y-shaped hexarotor
cascaded controller

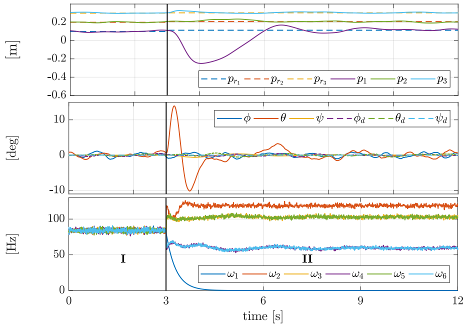

(healthy) tilted star-shaped hexarotor
non-linear controller

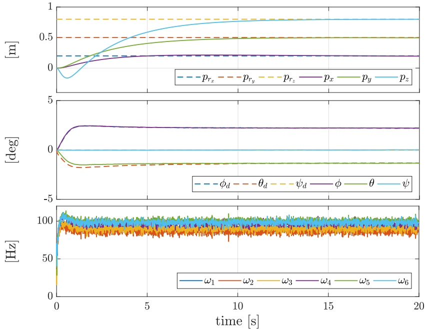

G. Michieletto, M. Ryll and A. Franchi. *Control of statically hoverable multi-rotor aerial vehicles and application to rotor-failure robustness for hexarotors.* IEEE International Conference on Robotics and Automation (ICRA), pp. 2747-2752, 2017.

G. Michieletto, A. Cenedese, L. Zaccarian, A. Franchi. *Nonlinear Control of Multi-Rotor Aerial Vehicles Based on the Zero-Moment Direction.* IFAC World Congress 2017, pp. 13686–13691, 2017.

Rigidity Theory for UAV Formation

relative bearing

$$\mathbf{b}_{ij} = \mathbf{R}_i^\top \frac{\mathbf{p}_j - \mathbf{p}_i}{\|\mathbf{p}_j - \mathbf{p}_i\|_2} = \mathbf{R}_i^\top \bar{\mathbf{p}}_{ij} \in \mathbb{S}^2$$

bearing function

$$\mathbf{b}_{\mathcal{G}} : SE(3)^n \rightarrow \mathbb{S}^{2^m}$$

$$\boldsymbol{\chi} \mapsto \mathbf{b}_{\mathcal{G}}(\boldsymbol{\chi}) = \left[\mathbf{b}_1^\top \dots \mathbf{b}_m^\top\right]^\top$$

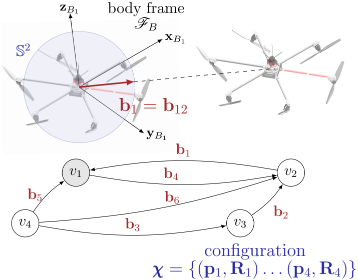

G. Michieletto, A. Cenedese, A. Franchi. *Bearing Rigidity Theory in SE(3).* IEEE 55th Conference on Decision and Control (CDC), pp. 5950-5955, 2016.

G. Michieletto, A. Cenedese. *SE(3) Bearing Rigidity Based Control for Fully-Actuated Systems.* IEEE 57th Conference on Decision and Control (CDC), submitted.

Rigidity Theory for UAV Formation

relative bearing

$\mathbf{b}_{ij} = \mathbf{R}_i^\top \frac{\mathbf{p}_j - \mathbf{p}_i}{\|\mathbf{p}_j - \mathbf{p}_i\|_2} = \mathbf{R}_i^\top \bar{\mathbf{p}}_{ij} \in \mathbb{S}^2$

bearing function

$\mathbf{b}_{\mathcal{G}} : SE(3)^n \to \mathbb{S}^{2^m}$

$$\boldsymbol{\chi} \mapsto \mathbf{b}_{\mathcal{G}}(\boldsymbol{\chi}) = \left[\mathbf{b}_1^\top \dots \mathbf{b}_m^\top\right]^\top$$

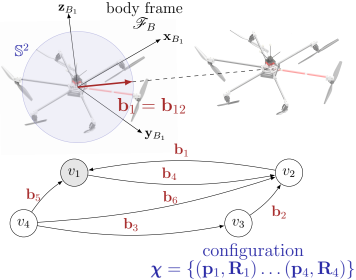

infinitesimal bearing rigidity

G. Michieletto, A. Cenedese, A. Franchi. *Bearing Rigidity Theory in SE(3).* IEEE 55th Conference on Decision and Control (CDC), pp. 5950-5955, 2016.

G. Michieletto, A. Cenedese. *SE(3) Bearing Rigidity Based Control for Fully-Actuated Systems.* IEEE 57th Conference on Decision and Control (CDC), submitted.

Rigidity Theory for UAV Formation

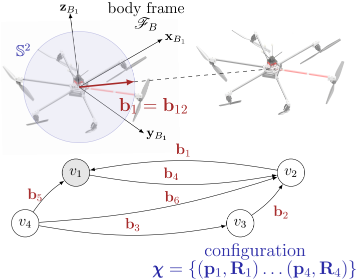

relative bearing

$$\mathbf{b}_{ij} = \mathbf{R}_i^\top \frac{\mathbf{p}_j - \mathbf{p}_i}{\|\mathbf{p}_j - \mathbf{p}_i\|_2} = \mathbf{R}_i^\top \bar{\mathbf{p}}_{ij} \in \mathbb{S}^2$$

bearing function

$$\mathbf{b}_\mathcal{G} : SE(3)^n \to \mathbb{S}^{2^m}$$

$$\boldsymbol{\chi} \mapsto \mathbf{b}_\mathcal{G}(\boldsymbol{\chi}) = \left[\mathbf{b}_1^\top \dots \mathbf{b}_m^\top\right]^\top$$

infinitesimal bearing rigidity

measurements maintenance $\propto$ rigidity matrix kernel

$$\dot{\mathbf{b}}_\mathcal{G}(\boldsymbol{\chi}) = \mathbf{B}_\mathcal{G}(\boldsymbol{\chi}) \begin{bmatrix} \mathbf{v} \\ \boldsymbol{\omega} \end{bmatrix} = \mathbf{0}$$

G. Michieletto, A. Cenedese, A. Franchi. *Bearing Rigidity Theory in SE(3).* IEEE 55th Conference on Decision and Control (CDC), pp. 5950-5955, 2016.

G. Michieletto, A. Cenedese. *SE(3) Bearing Rigidity Based Control for Fully-Actuated Systems.* IEEE 57th Conference on Decision and Control (CDC), submitted.

Rigidity Theory for UAV Formation

relative bearing

$$\mathbf{b}_{ij} = \mathbf{R}_i^\top \frac{\mathbf{p}_j - \mathbf{p}_i}{\|\mathbf{p}_j - \mathbf{p}_i\|_2} = \mathbf{R}_i^\top \bar{\mathbf{p}}_{ij} \in \mathbb{S}^2$$

bearing function

$$\mathbf{b}_\mathcal{G} : SE(3)^n \to \mathbb{S}^{2^m}$$

$$\boldsymbol{\chi} \mapsto \mathbf{b}_\mathcal{G}(\boldsymbol{\chi}) = \left[\mathbf{b}_1^\top \dots \mathbf{b}_m^\top\right]^\top$$

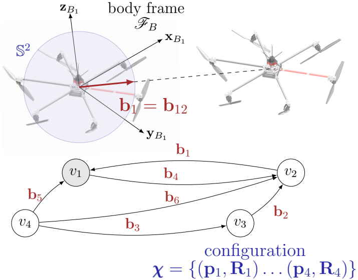

infinitesimal bearing rigidity

measurements maintenance $\propto$ rigidity matrix kernel

$$\dot{\mathbf{b}}_\mathcal{G}(\boldsymbol{\chi}) = \mathbf{B}_\mathcal{G}(\boldsymbol{\chi}) \begin{bmatrix} \mathbf{v} \\ \boldsymbol{\omega} \end{bmatrix} = \mathbf{0}$$

- IBR $\Leftrightarrow$ $rank(\mathbf{B}_\mathcal{G}(\boldsymbol{\chi})) = 6n - 7$

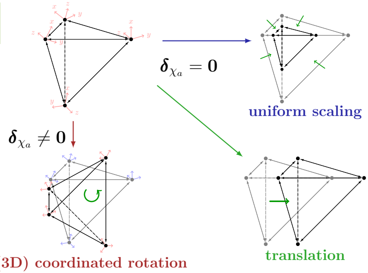

G. Michieletto, A. Cenedese, A. Franchi. *Bearing Rigidity Theory in SE(3).* IEEE 55th Conference on Decision and Control (CDC), pp. 5950-5955, 2016.

G. Michieletto, A. Cenedese. *SE(3) Bearing Rigidity Based Control for Fully-Actuated Systems.* IEEE 57th Conference on Decision and Control (CDC), submitted.

Stabilization and Control Applications

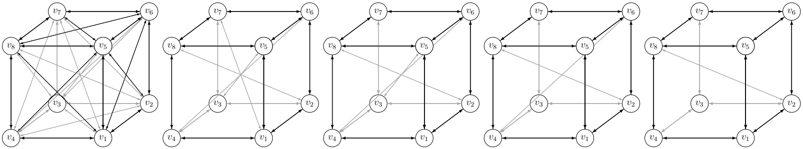

rigid formation stabilization:
desired bearing measurements achievement

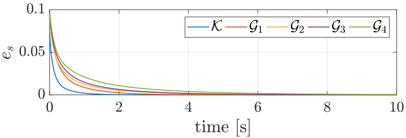

coordinated motion
along infinitesimally rigid trajectories

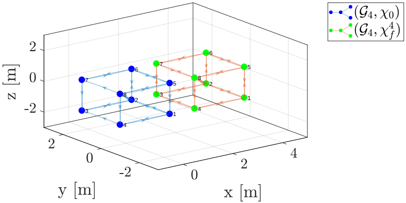

G. **Michieletto**, A. Cenedese, A. Franchi. *Bearing Rigidity Theory in SE(3).* IEEE 55th Conference on Decision and Control (CDC), pp. 5950-5955, 2016.

G. Michieletto, A. Cenedese. *SE(3) Bearing Rigidity Based Control for Fully-Actuated Systems.* IEEE 57th Conference on Decision and Control (CDC), submitted.

Summary

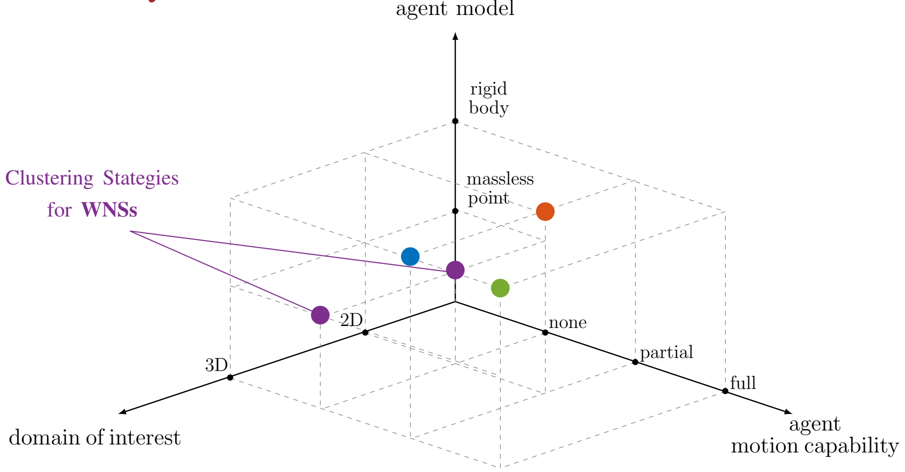
agent model
rigid body
massless point
Clustering Stategies for **WNSs**
2D
3D
none
partial
full
domain of interest
agent motion capability

Summary

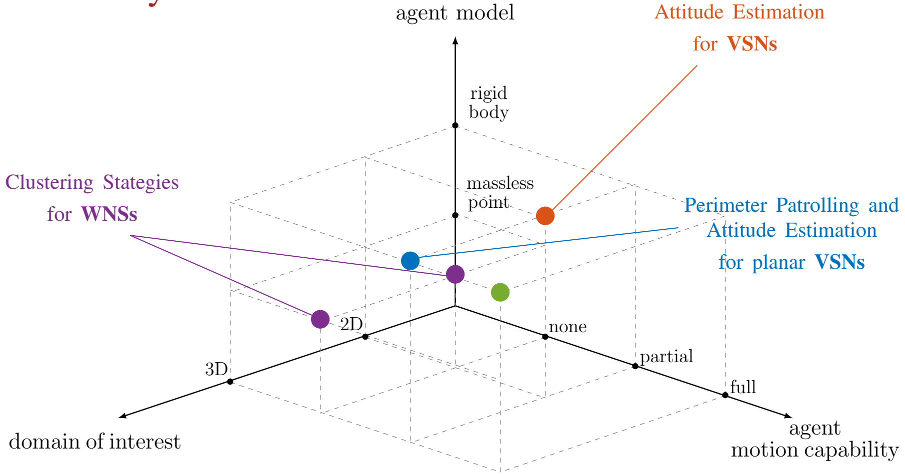
agent model
Attitude Estimation
for **VSNs**
rigid
body
massless
point
Clustering Stategies
for **WNSs**
Perimeter Patrolling and
Attitude Estimation
for planar **VSNs**
2D
3D
none
partial
full
domain of interest
agent
motion capability

Summary

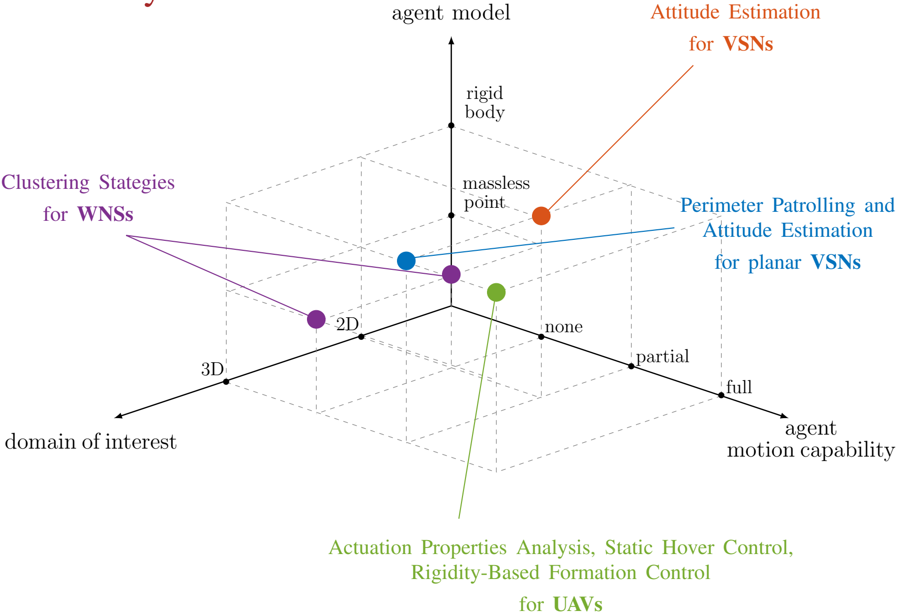
agent model
Attitude Estimation
for VSNs
rigid
body
massless
point
Clustering Stategies
for WNSs
Perimeter Patrolling and
Attitude Estimation
for planar VSNs
2D
3D
none
partial
full
domain of interest
agent
motion capability
Actuation Properties Analysis, Static Hover Control,
Rigidity-Based Formation Control
for UAVs

Thank you for your time!

Any questions?

Giulia Michieletto
Ph.D. Student
Dep. of Information Engineering
University of Padova, Italy

giulia.michieletto@unipd.it

DIPARTIMENTO DI INGEGNERIA DELL'INFORMAZIONE

SPARCS

Technology is morally neutral until we apply it